Supporting Information

Water Network

At very acidic pH values, aminoflavylium cations $\mathbf{AH^+}$ can protonate to form a dipositive flavylium ion $\mathbf{AH_2^{2+}}$. In the particular case of 4'-*N,N*-dimethylamino-7-hydroxyflavylium, the $\mathbf{AH_2^{2+}}$ absorbs at 430 nm and $\mathbf{AH^+}$ at 535 nm, which makes possible to observe a very strong color transition from yellow to pink when the pH is changed from -1 to 2, *see* Fig. 1S. The pK_{AH+} determined is -0.24.[1]

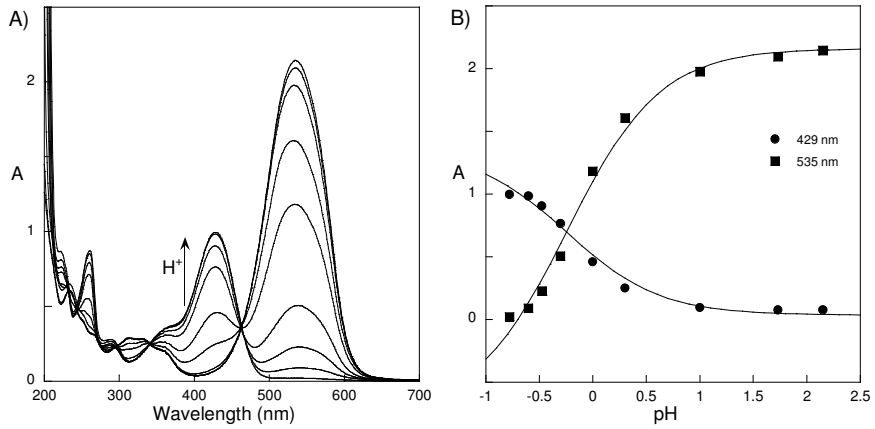

Fig. 1S – A) Spectra of solutions of [4'-*N,N*-dimethylamino-7-hydroxyflavylium] = 5x10^{-5}M at 6M, 4M, 3M, 2M, 1M HCl and at pH 1.0, 1.73 and 2.15. B) Fitting of the absorptions at 535 and 429 nm was achieved with pK_{AH+} value of -0.24.

When the pH is increased, deprotonation of the aminoflavylium cation $\mathbf{AH^+}$ to form the quinoidal base **A** takes place. The spectra of both species is highly overlapped making difficult the determination of the pK_a value, *see* Figure 2S. Although the experimental error is significant, a pK_a value around 5.4±0.2, can be determined.

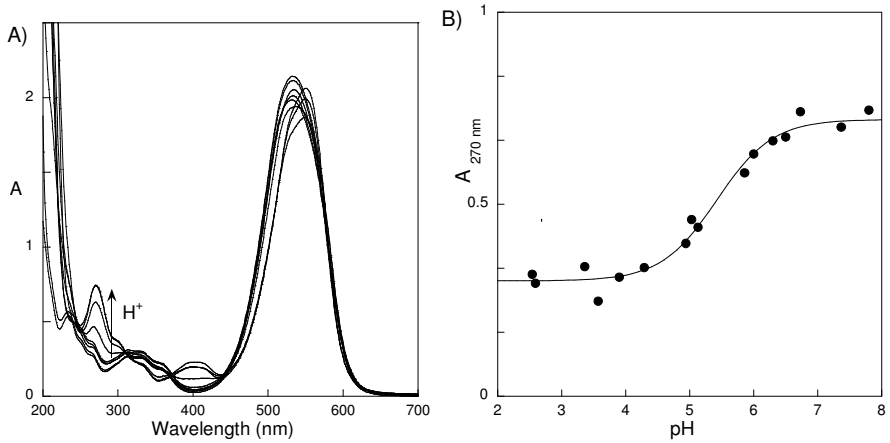

Fig. 2S – A) Immediate spectra of solutions of [4'-*N,N*-dimethylamino-7-hydroxyflavylium] = 5x10^{-5} M after a pH jump from 1 to 4.29,4.94, 5.03, 5.13, 5.86, 6.00, 6.30, 6.50, 6.73, 7.37, 7.80 and 8.20 (not all spectra shown). B) Fitting of the absorptions at 500 nm was achieved with pK_a value of approximately 5.4.

At very basic pH values the thermodynamic stable species are the ionized *trans*-chalcones. If the titration of a dionized chalcone $\mathbf{Ct^{2-}}$ to acidic pH values is performed, the species $\mathbf{Ct^{-}}$ and **Ct** are obtained, *see* Figure 3S. In this case values of pK_{Ct1} and pK_{Ct2} are 8.1 and 9.6, respectively, *see* Fig 3S. The **Ct** species has maximum absorption at 410 nm and the $\mathbf{Ct^{2-}}$ species at 490 nm.

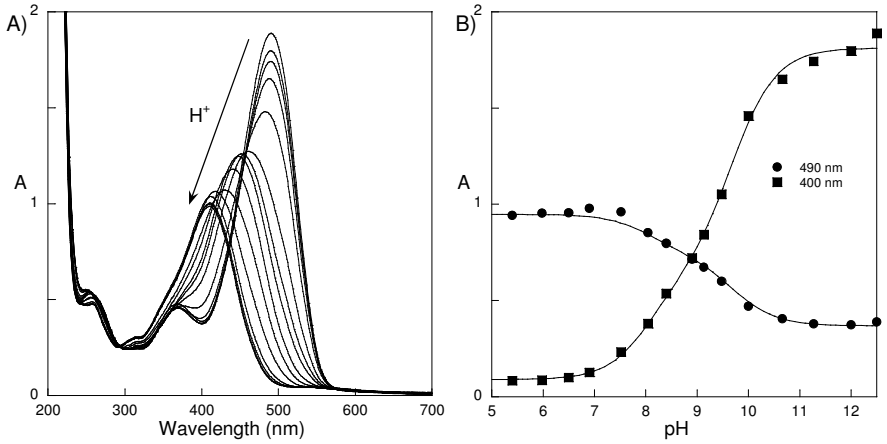

Fig. 3S – A) Spectra of solutions of [4'-*N,N*-dimethylamino-7-hydroxyflavylium] = $5x10^{-5}$ M from pH 12.5 to pH 4, obtained by successive acidification of the thermally equilibrated solution at pH 12.5. B) Fitting of the absorptions at 400 and 490 nm was achieved with pK_{Ct1} and pK_{Ct2} values of 8.1 and 9.6.

The **Ct** species, in the case of aminoflavylium compounds can also protonate to give a $\mathbf{CtH^{+}}$ species whose absorption spectrum exhibits a maximum *ca.* 370 nm. However, this not the thermodynamically stable species giving rise to the flavylium ion in water. In order to obtain the respective pK_{Ct+} value, a series of pH jumps from very basic (equilibrated) solutions was performed and the spectra registered immediately after (before significant conversion into $\mathbf{AH^{+}}$), allowing to obtain an estimative of the pK_{Ct+} of 2.3, Fig. 4S.

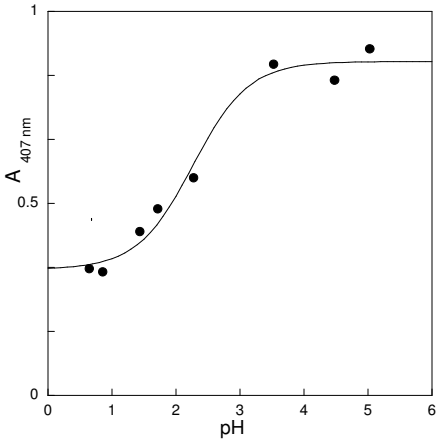

Fig. 4S –Fitting of the absorptions at 407 nm (Ct species) as a function of the final pH value of a pH jump from a stock solution at pH around 13 was achieved with pK_{Ct+} of 2.3.

The final equilibrated solutions shows the presence of two species $\mathbf{AH^+}$ and **Ct**, as well as **A**, thus being possible to define an equilibrium K'_a, eq.(1) of the manuscript. This **Ct** species presents a great tendency to precipitate in water solutions, and the pK'_a value had to be evaluated in very diluted solutions. This value was determined at room temperature 20 ± 1ºC (pK'_a = 4.4, *see* Fig. 5S) and at 60 ºC (pK'_a = 4.2).

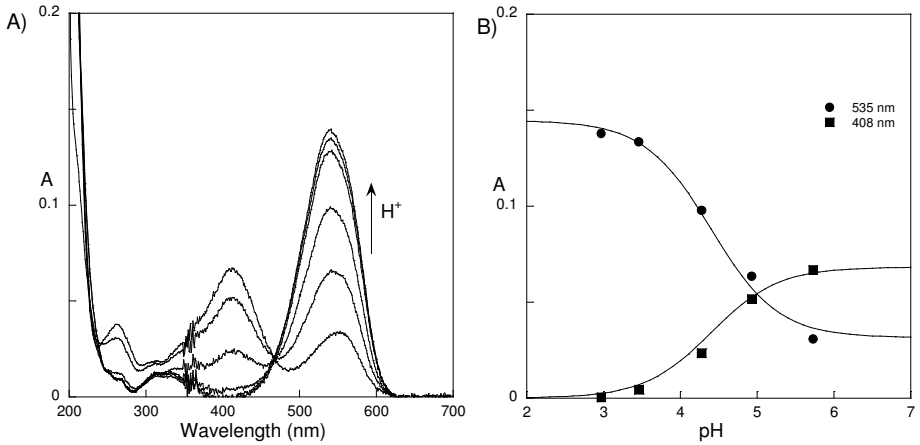

Fig. 5S – A) Spectra of equilibrated solutions of [4'-*N,N*-dimethylamino-7-hydroxyflavylium] = 3.6×10^{-6} M at pH 2.22, 2.97, 3.46, 4.28, 4.93, 5.73 at room temperature. B) Fitting of the absorptions at 535 and 408 nm was achieved with pK'_a of 4.4.

In order to confirm the previous pK_a ($\mathbf{AH^+/A}$) value a pH jump from 1 to 6.9 was performed and ratio of the amplitudes of the initial and final absorption at 550 nm was found to be 0.159. Taking into account that % A = K_a/K'_a and pK'_a = 4.4, a value of pK_a of 5.2 is obtained, which is in a very reasonable agreement with the experimental data depicted in Fig. 2S.

In order to get some insight into the kinetics of the process, the kinetics of pH jumps from a stock solution at very basic pH values ($\mathbf{Ct^{2-}}$) to acidic pH values were followed at room temperature. The results obtained are plotted in Fig. 6S and can be interpreted considering two regimes: i) one that gives the $\mathbf{AH^+}$ from **Ct** (moderately acidic pH values) and with which a bell shaped curve is predicted, eq. (1S), ii) other that gives the $\mathbf{AH^+}$ from $\mathbf{CtH^+}$, at very acidic pH values, eq. (2S).[1]

$$A \underset{}{\overset{K_a}{\rightleftharpoons}} AH^+ \underset{k_{-h}[H^+]}{\overset{k_h}{\rightleftharpoons}} B \overset{K_t}{\rightleftharpoons} Cc \underset{k_{-i}}{\overset{k_i}{\rightleftharpoons}} Ct$$

$$k_{obs} = \frac{\frac{[H^+]}{[H^+]+K_a} k_i K_t \frac{k_h}{k_{-h}} + k_{-i}[H^+]}{[H^+]+\frac{k_i K_t}{k_{-h}}} \qquad (1S)$$

$$CtH^+ \underset{k_{i+}}{\overset{k_{-i+}}{\rightleftharpoons}} X' \xrightarrow{k_{-h+}[H^+]} AH^+$$

$$k_{obs} = \frac{\dfrac{[H^+]}{[H^+]+K_{Ct+}} k_{-i+}[H^+]}{[H^+]+\dfrac{k_{i+}K_{t+}}{k_{-h+}}} \qquad (2S)$$

The expected trend is obtained and it is possible to evaluate the order of magnitude of the kinetics of the process under study, Fig. 6S.

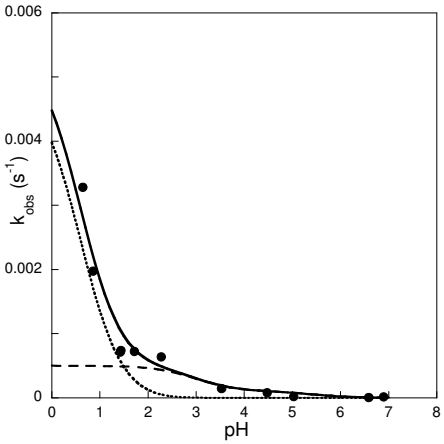

Fig. 6S – Kinetics of pH jumps from a stock solution at very basic pH values (**Ct**$^{2-}$) to acidic pH values were followed at room temperature**.** Fitting, full line, was achieved by a sum of eq. 1S (traced line) and eq. 2S (pointed line) – pK_{Ct+}=2.3, k_{-i+} = 5x10^{-3} s^{-1}, $k_{i+}K_{t+}/k_{-h+}$ = 0.25 M, pK_a = 5.45, $k_iK_tK_h$ = 1x10^{-7} s^{-1}, k_{-i} = 5x10^{-4} s^{-1}, $k_{-i}K_T/k_{-h}$ = 1x10^{-3} s^{-1} M^{-1}.

Fluorescence studies were also performed on equilibrated solutions. A fluorescence maximum, when exciting at 540 nm, is obtained at 608 nm that could be due to the flavylium cation or the base. However, the increasing intensity of this fluorescence with increasing pH values discards the **AH**$^+$ emission. The trend of the emission can thus be attributed to the **A** species that is in equilibrium with **Ct**. The observed pK^*_a =4.3 corroborates this interpretation (pK'_a = 4.4), *see* Fig 7S.

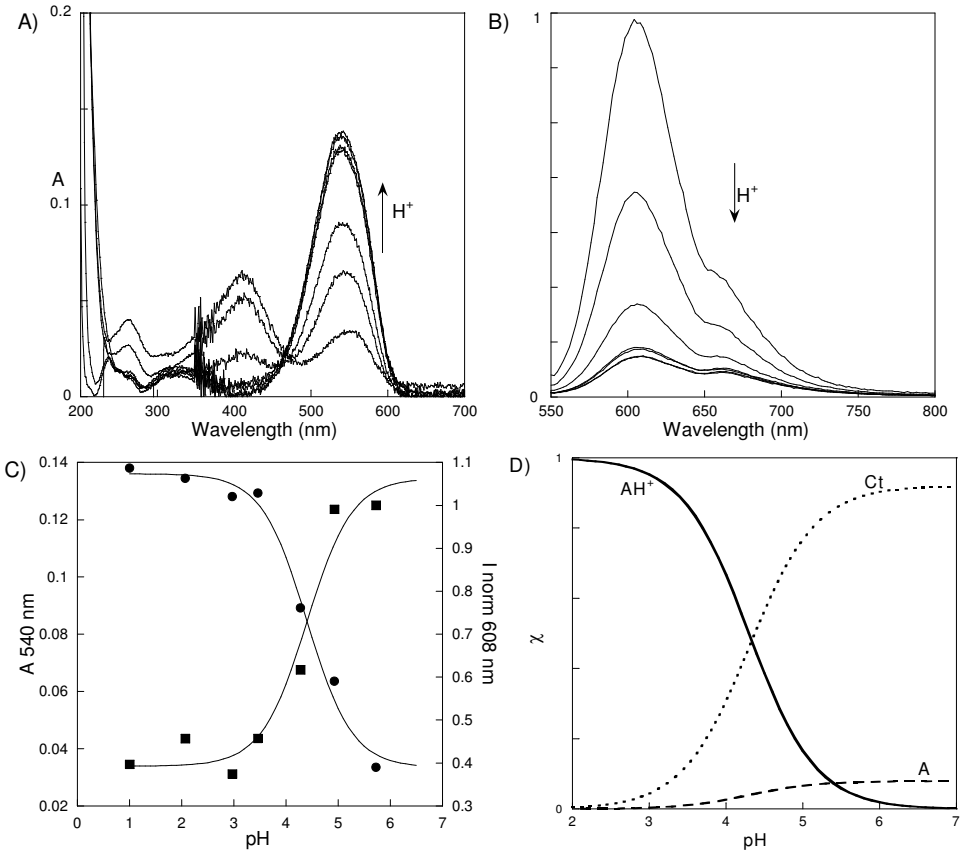

Fig. 7S – A) Absorption spectra of equilibrated solutions at pH 1, 2.07, 2.97, 3.46, 4.28, 4.93 and 5.73. B) Emission spectra of the same solutions exciting at 540 nm. C) Plot of the absorbance at 540 nm and intensity of fluorescence versus pH. D) Molar Fractions of Ct, AH^+ and A in equilibrium – the low percentage of A is responsible for the emission observed.

pK'_a Pluronic gels and micelles

The equilibrium distribution and the pK'_a, eq.(1), are affected by preferential stabilization of one of the species takes place. The pK'_a in water is practically independent on the temperature. In the presence of the Pluronic (at any concentration) the acidity constant always increases because **Ct** is (relatively to **AH$^+$**) stabilized by the polymer. In the case of 1.5% of Pluronic the dependence is approximately a sigmoid with a transition that is compatible with a critical micelle temperature (CMT) of 28.5 ^{0}C as previously reported.[2] At 30 % of Pluronic the pK'_a reaches a plateau which is only compatible with a sol-gel transition that was previously reported in literature to occur at ca. 18 ^{0}C.[3] However, the pK'_a in the presence of micelles formed at lower temperature for 30% of polymer is higher than the one observed at higher temperature for 1.5 % of polymer. This behavior can be explained if the decreasing of polarity in the water phase, by increasing polymer concentration is taken into account. It is known that flavylium cation is more soluble in ethanol than in water, and by consequence it could be expected a stabilization of **AH$^+$** at 30% of Pluronic when compared with 1.5 %, as shown in Fig.8SA.

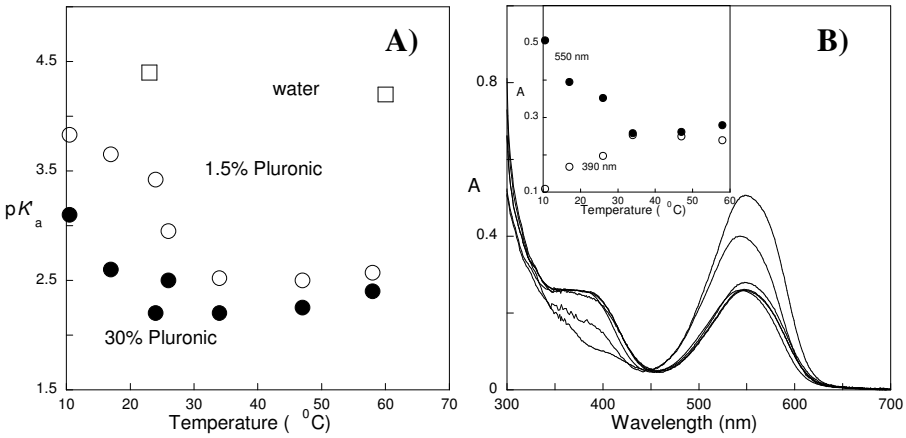

Fig. 8S – A) pK'_a vs. temperature for water, (□), 1.5 %(○) and 30% (●) of Pluronic. B) Spectral variations of the compound 4'-*N,N*-dimethylamino-7-hydroxyflavylium in the presence of Pluronic F127 30% at pH=2.6, as a function of temperature.

However, at pH=2.6 (30% of Pluronic), Fig 8SB the equilibrium that is established between **AH$^+$/A** and **Ct** is clearly shifted by raising the temperature, and the fraction of **Ct** is increased at the expenses of **AH$^+$/A**. In other words, the shift of the equilibrium towards **Ct** is a result of the increasing of the less polar environment surrounding **Ct**, as expected if the gel is formed, the phase transition taking place at *ca.* 18 ^{0}C, see inset of Fig. 8SB. At this polymer concentration the micelles are already formed at the lower temperature and by consequence the observed changes can be attributed to the gel formation.

Inspection of the inset of Fig. 8SB indicates that the equilibrium between **Ct** and **AH^+/A** can be used as a sensor to determine the critical gel temperature.

Photochemistry in Pluronic gels and micelles

Either in the presence of micelles of Pluronic F127 (1.5%) or incorporated in a gel (30%), the uncolored **Ct** species gives rise to the formation of the pink-red **AH^+** or **A** species, upon irradiation. The system is completely reversible in a time scale that depends on pH, temperature and percentage of polymer used. In Fig. 9S, some details of these photochromic reversible systems are shown.

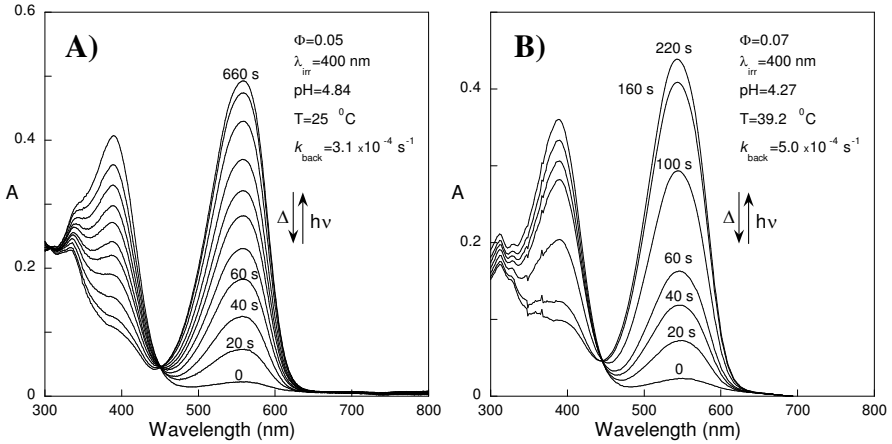

Fig. 9S. – A) Spectral variations of the compound 4'-*N,N*-dimethylamino-7-hydroxyflavylium incorporated in a 30 % Pluronic F127 gel. B) Spectral variations of the compound 4'-*N,N*-dimethylamino-7-hydroxyflavylium dissolved in micelles of Pluronic F127 (1.5%).

Traces of the transient absorptions after flash of the compound 4'-*N,N*-dimethylamino-7-hydroxyflavylium in the presence of the gel (Pluronic F127, 30%, 45 ^{0}C,) are shown in Fig. 10S. Identical traces were obtained for micelles (1.5% of the Pluronic F127, 45 ^{0}C). The transients were monitored at 400 nm (**Ct**) and 540 nm (**AH^+**). Two parallel processes following the same first order rate constant take place: one leading to the formation of the photoproduct and the other recovering (partially) the **Ct**. As shown previously[4] the experimental results can be accounted for by eq.(3S)

$$K_{flash} = k_i^m \frac{K_t^m}{1+K_t^m} + \frac{k_{-h}^m}{1+K_t^m}\left[H^+\right] \qquad (3S)$$

Where the superscript m refers that all the events monitored by the flash photolysis occur inside the micellar envrironment, the other rate constants being defined in Scheme 1, and the equilibrium constant defined as $K_t^m = \frac{k_t^m}{k_{-t}^m}$.

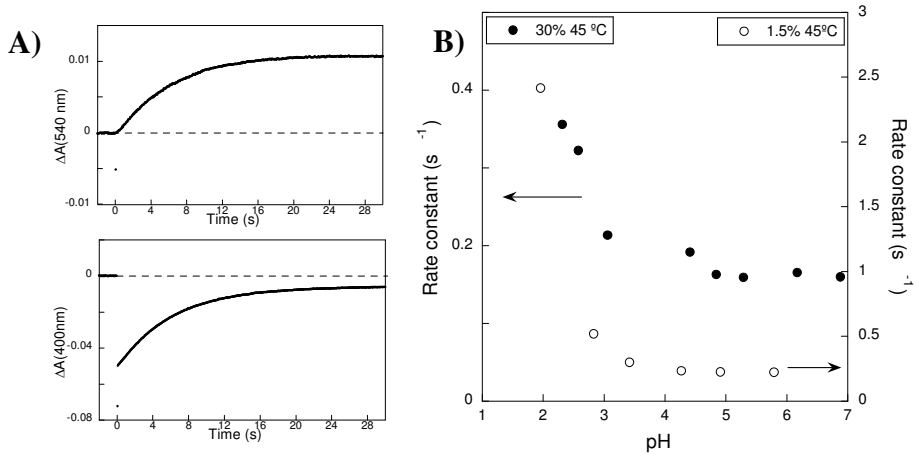

Fig. 10S – A) Transient absorption traces of the **Ct** (400 nm) and $\mathbf{AH^+}$ species (540 nm), pH=5.3 T=45 ^{0}C for a gel 30 % Pluronic F127, both curves decay with the same rate constant. B) Plot of the rate constants obtained at 45 ºC, for 30 % Pluronic F127 (gel ●) and 1.5 % Pluronic F127 (micelles ○).

In eq.3S the first term accounts for the recovering of **Ct** while the second, which is proton dependent refers to the process leading to the photoproduct. According to the model[4] once $\mathbf{AH^+}$ is formed it is expelled to the hydrophobic environment where it is more soluble. Fitting of the date reported in Fig. 10S allows to construct Table 1S.

Tab. 1S – Parameters from the fittings of experimental points in Fig. 10SB with eq. 3S.

T=45 ^{0}C	**1.5% F-127 micelles**	**30% F-127 gel**
$k_i^m \frac{K_t^m}{1+K_t^m}$ (s^{-1})	0.22	0.17
$\frac{k_{-h}^m}{1+K_t^m}$ (M^{-1}s^{-1})	200	43

Fluorescence quantum yields in different media

Tab. 2S – Fluorescence quantum yields in different media.

	AH^+	Ct	A	Ct^{2-}
water	0.05 %	0.05 %	0.3 %	0.2 %
Organic media		Methanol 0.1 % Ethanol 0.4 % Decanol 0.8 %	Methanol 8 % Ethanol 30 % Decanol 36 %	
Viscous Media	Sucrose (67 %) aqueous solution 2 %	Glycerol 2.5 %		
Pluronic 20 % **(gel,40 ºC)**	0.5 %	0.5 %	18 %	

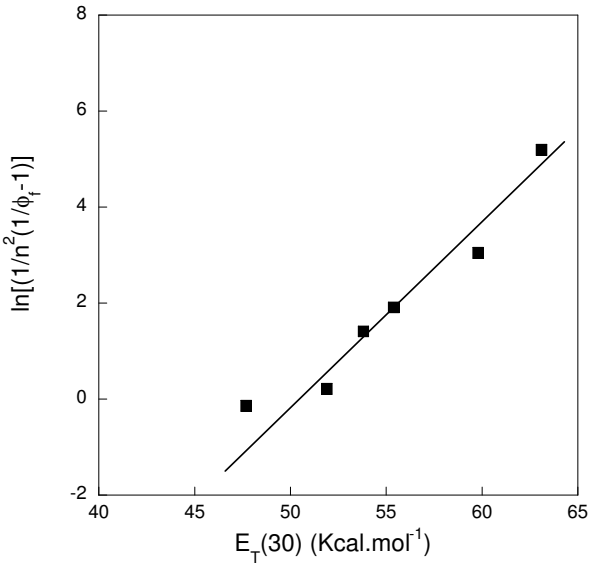

Fig. 12S – $\ln[1/n^2(1/\phi_f-1)]$ for **A** species in protic solvents as a function of $E_T(30)$.

Flash photolysis in pure solvents

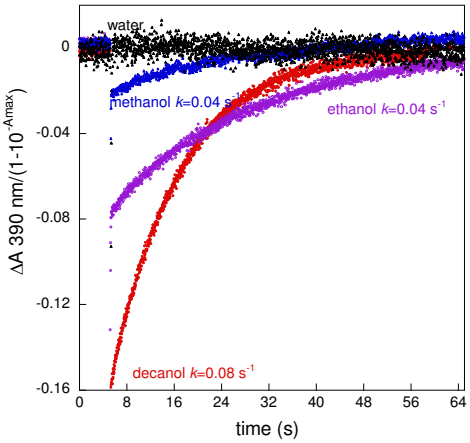

Fig. 13S – Flash photolysis traces obtained in water, methanol, ethanol and decanol, following the variation in absorption at 390 nm. First order rate constants are shown.

REE Ct in Methanol

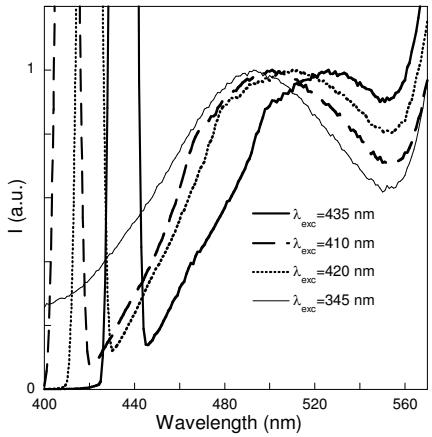

Fig.14 S –Emission spectra of the compound 4'-*N,N*-dimethylamino-7-hydroxyflavylium (**Ct** form) in methanol at different excitation wavelengths.

Absence of REE in A species

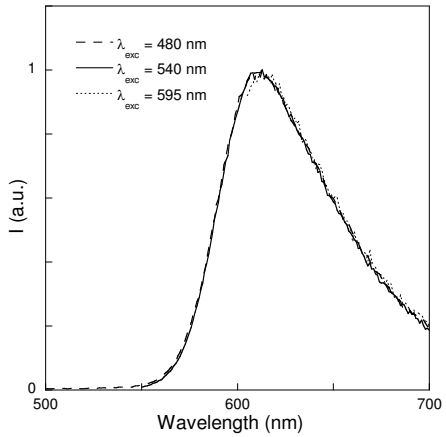

Fig. 15S –Emission spectra of the compound 4'-*N,N*-dimethylamino-7-hydroxyflavylium (**A** form) in Pluronic gel, F127 20 %, at 40 ºC, pH=5.9 at different excitation wavelengths

Analysis of fluorescence decays

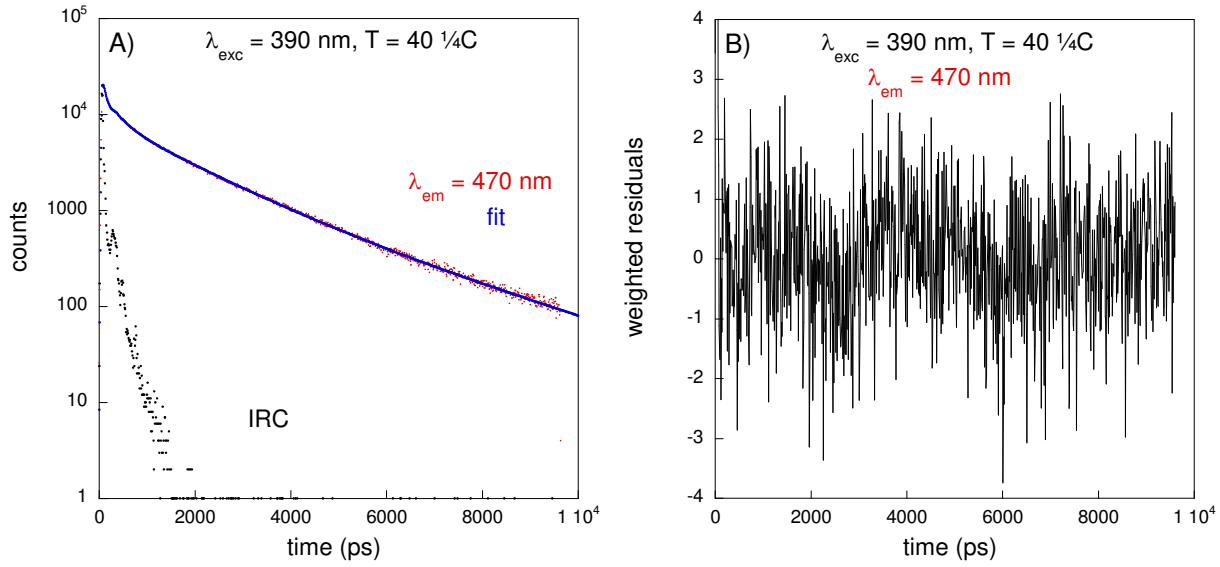

Fig. 16S –A) Fluorescence decay 20 % Pluronic F127, pH 5.9, λ_{exc}=390 nm, λ_{em}=470 nm, T=40 ºC in PSS (10 ps/channel) and respective fitting. B) Weighted residuals for the fit in A) (for details see Table 3).

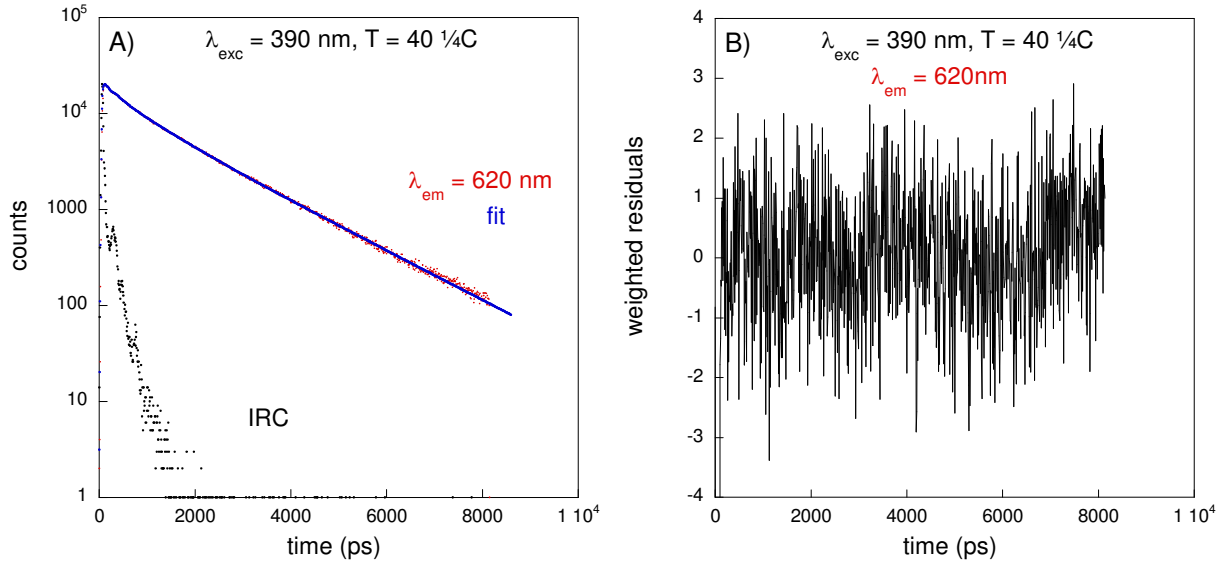

Fig. 17S –A) Fluorescence decay 20 % Pluronic F127, pH 5.9, λ_{exc}=390 nm, λ_{em}=620 nm, T=40 ºC in PSS (8.4 ps/channel) and respective fitting. B) Weighted residuals for the fit in A) (for details see Table 3).

Analysis of fluorescence anisotropy decays

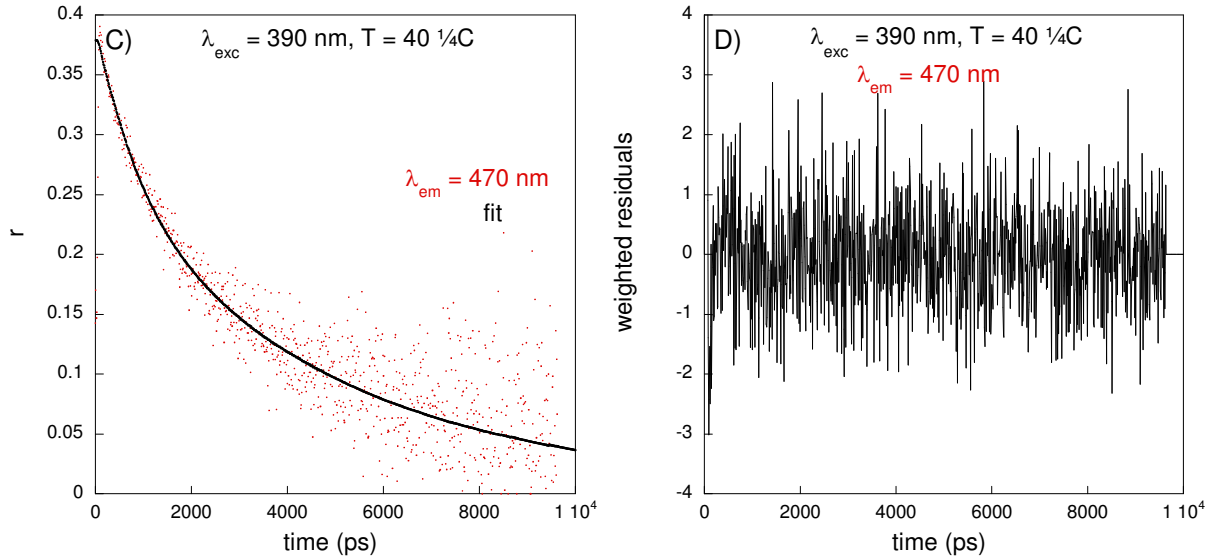

Fig. 18S –A) Fluorescence anisotropy decay 20 % Pluronic F127, pH 5.9, λ_{exc}=390 nm, λ_{em}=470 nm, T=40 ºC in PSS (10 ps/channel) and respective fitting. B) Weighted residuals for the fit in A) (for details see Table 3).

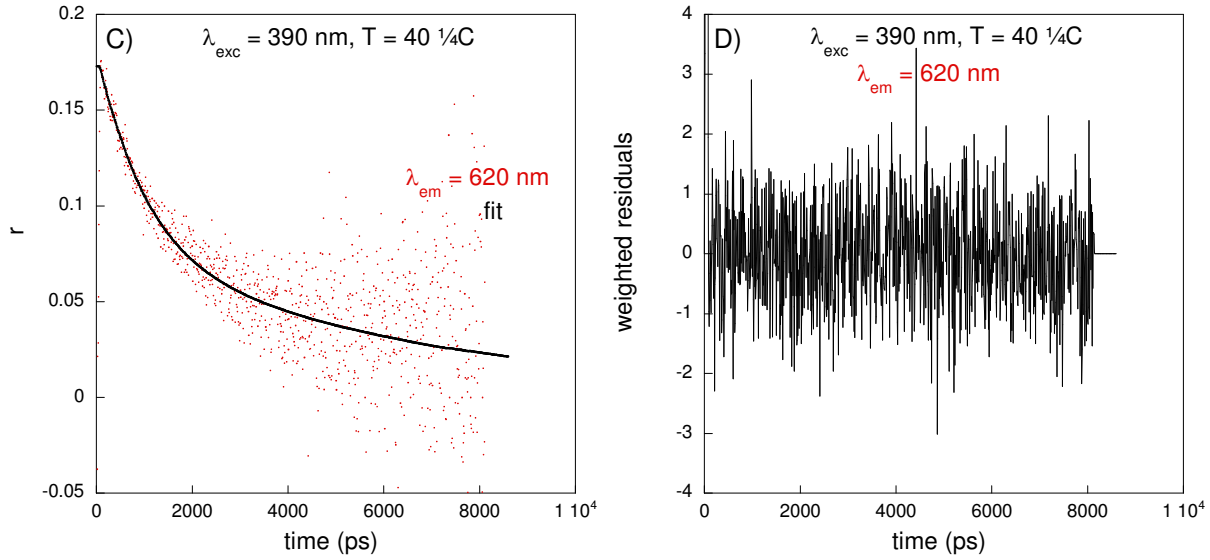

Fig. 19S –A) Fluorescence anisotropy decay 20 % Pluronic F127, pH 5.9, λ_{exc}=390 nm, λ_{em}=620 nm, T=40 ºC in PSS (8.4 ps/channel) and respective fitting. B) Weighted residuals for the fit in A) (for details see Table 3).

[1] Moncada, M. C.; Fernandez, D.; Lima, J. C.; Parola, A. J.; Lodeiro, C.; Folgosa, F.; Melo, M. J.; Pina, F. *Org. Biomol. Chem.*, **2004**, 2, 2802-2808.
[2] Pina, F.; Hatton, T. A. *Langmuir* **2008**, 24, 2356-2364.
[3] Alexandridis, P.; Hatton, T. A. *Colloids Surfaces A: Physicochem. Eng. Aspects* **1995**, 96, 1-46.
[4] Gomes, R.; Parola, A. J.; Laia, C. A. T.; Pina, F. *Photochem. Photobiol. Sci.* **2007**, 1003-1009.